



Open Archive TOULOUSE Archive Ouverte (OATAO)

OATAO is an open access repository that collects the work of Toulouse researchers and makes it freely available over the web where possible.

This is an author-deposited version published in : <http://oatao.univ-toulouse.fr/>
Eprints ID : 16509

To link to this article : DOI: 10.1109/ICEP.2016.7486818
URL : <http://dx.doi.org/10.1109/ICEP.2016.7486818>

To cite this version : Libot, Jean-Baptiste and Arnaud, Lionel and Dalverny, Olivier and Alexis, Joël and Milesi, Philippe and Dulondel, Frédéric *Mechanical fatigue assessment of SAC305 solder joints under harmonic vibrations*. (2016) In: 2016 International Conference on Electronics Packaging (ICEP 2016), 20 April 2016 - 22 April 2016 (Sapporo, Japan).

Any correspondence concerning this service should be sent to the repository administrator: staff-oatao@listes-diff.inp-toulouse.fr

Mechanical fatigue assessment of SAC305 solder joints under harmonic vibrations

J.B. Libot^{1,2}, L. Arnaud¹, O. Dalverny¹, J. Alexis¹, P. Milesi², and F. Dulondel²

¹ University of Toulouse; INP/ENIT; LGP; 47, avenue d'Azereix; F-65013 Tarbes, France

² SAFRAN Sagem; 21, avenue du gros chêne, F-95610 Eragny-sur-Oise, France

Abstract—Vibration-induced solder joint fatigue is a main reliability concern for aerospace and military industries whose electronic equipment used in the field is required to remain functional under such loading. Due to the RoHS directive which eventually will prevent lead from being utilized in electronic systems, there is a need for a better understanding of lead-free mechanical behavior under vibration conditions. This study reports the durability of Sn3.0Ag0.5Cu (SAC305) solder joints subjected to harmonic solicitations at three specific temperatures (-55°C, 20°C and 105°C). A test assembly is designed and consists in a single daisy-chained 1152 I/O ball grid array (FBGA1152) package assembled on a flame retardant (FR-4) printed circuit board (PCB). The vibration levels are imposed by a controlled deflection at the center of the board at its natural frequency. The electric continuity is monitored to determine the number of cycles to failure of each sample. Mode shape measurements with a scanning vibrometer are also conducted and correlated with Finite Element Analysis (FEA) to ensure accurate calculation of stress within the critical solder balls at the corners of the component. The failed specimens are then cross-sectioned in order to determine failure modes. A comparison of SAC305 durability with SnPb36Ag2 solder is given, along with a set of lifetime measurements for two complementary assemblies: 68 I/O Leadless Chip Carrier (LCC68) and 324 I/O Plastic Ball Grid Array (PBGA324). It turns out that SAC305 outperforms SnPb36Ag2 and the effect of temperature on the mechanical durability of SAC305 appears to be minor. Failure analysis points out different failure modes such as ductile and brittle cracks at the interface between the solder bulk and the component, along with pad cratering-induced copper trace failures. FEA calculations provide data to estimate the high cycle fatigue (HCF) behavior of SAC305 solder under harmonic vibrations.

Keywords—SAC305 solder; harmonic vibrations; FEA; Fatigue

I. INTRODUCTION

Electronic equipment for aerospace and military applications can encounter a wide range of environmental stresses mainly due to temperature variations, vibrations and shocks [1]. While most of the published work focuses on thermal cycling reliability, an increasing number of researchers have studied lead-free solder joint durability under dynamic loadings. With the RoHS directive preventing the use of lead (Pb), lead-free solder joint fatigue in severe vibration environments has especially become a great concern in electronic industry. The carried out studies have mainly focused on mechanical durability of BGA packages at room temperature. Kim et al. developed a torsional vibration fatigue machine allowing mixed mode stresses to occur in BGA solder

balls and assessed the vibration fatigue life of Pb-Sn (SnPb36Ag2) and Pb-free joints (SAC105) [2]. Chen et al. assessed the sinusoidal vibration durability of a PBGA component using a linear cumulative damage rule (Miner's rule) combined with empirical tests and FEA [3]. Che et al. used quasi-static and harmonic analysis along with experimental data to predict flip chip solder joint reliability (tin-lead eutectic solder) under harmonic vibrations [4]. Zhou et al. used mechanical bending and vibration tests to compare the low (LCF) and high cycle fatigue (HCF) of SAC305 and Pb-Sn solder joints [5].

The present work aims to assess the isothermal durability of SAC305 solder joints under harmonic vibrations at different temperatures (-55°C, 20°C and 105°C). Three test vehicles were designed using FBGA1152, PBGA324 and LCC68 packages mounted on an FR-4 printed circuit board. The experimental procedure consisted in performing out-of-plane sinusoidal vibrations at the natural frequency of each test boards until failure. The deflection at the center of the assembly was chosen as the loading parameter and the input acceleration levels were thus chosen accordingly. Scanning vibrometer and global-local FEA were combined to determine stress in the critical solder ball at the corner of the component. The results were correlated with the experimental data from vibration fatigue tests to plot a SAC305 polycyclic fatigue curve. A comparison is made between the harmonic durability of SAC305 and SnPb36Ag2 solder alloy for one specific loading level. A correlation is also made between the unidirectional printed circuit board curvature and the central deflection of the board. Several failure mechanisms can be observed under vibration solicitations as reported by different authors [5,6]. An in-depth failure analysis was thus conducted in order to determine the main failure modes induced by the tested dynamic loadings.

II. HARMONIC TESTS

A. Test vehicles and setup

Three test vehicles with three different components are designed for this study (Fig. 1). The substrate is a 110 x 110 mm, 1.6 mm thick FR-4 printed circuit board on which is assembled a single component at its center. The board is drilled with 8 holes allowing the fixture of the assembly at each corner on the electrodynamic shaker. The distance between inner holes is 70 mm and the distance between outer holes is 90 mm. The board has Electroless Nickel Immersion Gold (ENIG) surface finish on non-solder mask defined (NSMD) pads. The components are chosen according to their size, their type

(matrix or peripheral array packages) and associated solder shapes. A 35x35 mm FBGA1152 component is assembled with 0.5 mm diameter SAC305 or SnPb36Ag2 solder balls (with SAC305 and SnPb36Ag2 solder paste respectively) in 1 mm pitch. It has a nickel gold (Ni/Au) finish on solder mask defined (SMD) pads (Fig.1.a)). The second test assembly consists in a peripheral 24.1x24.1 mm LCC68 package mounted on the FR-4 board with SAC305 solder paste in 1.27 mm pitch (Fig.1.b)). Another matrix array package is considered as a 19x19 mm PBGA324 is soldered on the PCB with 0.5 mm diameter SAC305 solder balls and solder paste in 1 mm pitch. It has a Ni/Au finish on SMD pads (Fig.1. c)).

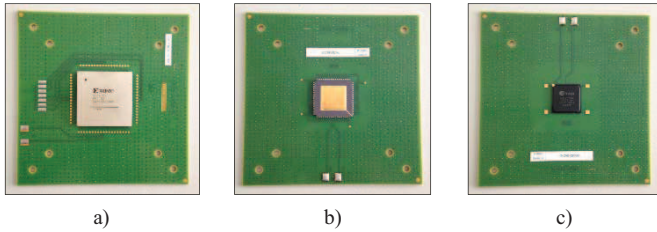


Fig. 1. Test vehicles assembled with a) FBGA1152, b) LCC68 and c) PBGA324.

All these three packages are daisy-chained in order to detect failures in the interconnections during vibration tests. The daisy-chain resistance is not continuously monitored throughout the test but the assembly is connected to the safety channel of the high speed data acquisition system which is able to detect any micro electrical breakdown with a precision of detection to microsecond. The first total crack in a solder joint will therefore automatically lead to the electrodynamic shaker stoppage, allowing the determination of the time to failure.

The experimental apparatus used for this study is given in Fig. 2. The isothermal fatigue tests are performed using an electrodynamic shaker placed in a thermal chamber and combined with a vibration control testing facility using LMS Test.Lab software. The thermal chamber can generate temperatures ranging from -55°C to 105°C. The electrodynamic shaker used for this study can produce out-of-plane acceleration up to 60 g ($1 \text{ g} = 9.81 \text{ m.s}^{-2}$).

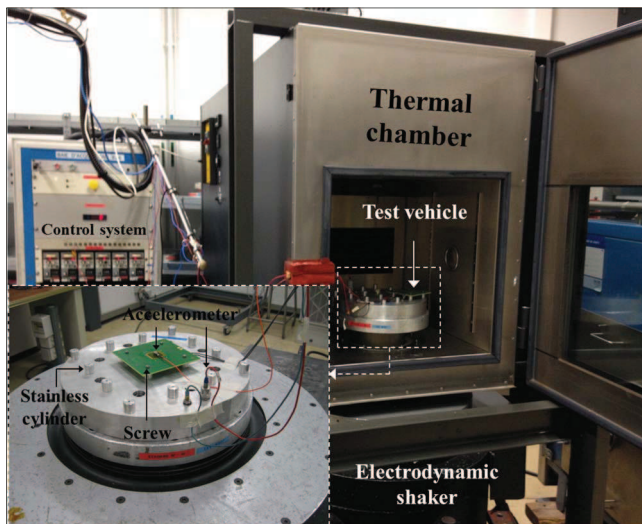


Fig. 2. Experimental setup for isothermal vibration tests.

The temperature range is selected according to typical temperatures observed in aerospace and military environments. The test specimen is fixed on 16 mm diameter stainless cylinders at each corner of the assembly with a 70 mm space between each fixture. The torque applied on the A4 stainless 3 mm diameter screws is set to 0.75 N.m before each testing for repeatability purpose and so, even at extreme temperatures once the thermal equilibrium is reached. Two accelerometers are placed on the fixture and on the test vehicle to determine the dynamic response of the assembly.

B. Test procedure and matrix

The loading parameter for the harmonic vibration assessment is the deflection at the center of the board at its natural frequency. This displacement d can be determined from the response of the accelerometer placed at the center of the test assembly using the following equation

$$d(t) = \frac{a_c(t)}{4\pi^2 f_0^2} \quad (1)$$

where $a_c(t)$ is the board acceleration response and f_0 the natural frequency of the test assembly. The harmonic vibration tests are conducted following two main steps. First, an experimental modal analysis is run to determine the natural frequency of the test specimen. Then, using (1), the assembly is subjected to sinusoidal forced vibrations with an imposed central displacement at the natural frequency until the first solder failure is detected. The vibration control system combined with the LMS Test.Lab software allows the tracking of the natural frequency so that any shift is corrected throughout testing. Table 1 gives the test matrix corresponding to the sinusoidal vibration tests carried out in this study (d_0 is the reference central deflection). The isothermal tests at -55°C and 105°C are conducted following the same procedure except that a 40 minutes delay is observed once the desired temperature is reached to account for thermal inertia.

TABLE I. TEST MATRIX

Solder	Package	d/d_0	T (°C)	Test specimen
SAC305	LCC68	1.50	20	8
		1.67	20	12
	PBGA324	1.00	20	12
		1.33	20	12
	FBGA1152	0.50	20	16
			-55	12
		0.57	20	16
			0.62	20
		0.67	20	16
			-55	12
		0.83	20	16
			105	12
		1.00	20	16
		1.17	105	12
1.33	20	16		
SnPb36Ag2	FBGA1152	0.83	20	16

A minimum of 12 test assemblies per loading condition (except for one configuration where 8 samples were tested) are used to get a statistical distribution of lifetime results. The number of cycles to failure is calculated by multiplying the time to failure by the natural frequency of the test vehicle.

III. SCANNING VIBROMETER MEASUREMENTS

In order to accurately capture the stress in the critical solder joint, it is necessary to determine the out-of-plane displacement of the test assembly. The solder joint which is the more likely to fail during vibration testing is the outermost solder joint at the corner of the component as reported by several authors [7,8]. Uniaxial modal deflections are thus measured in the diagonal of the test vehicle using a Polytec PSV-500 scanning vibrometer. Modal deflections are determined for 6 configurations corresponding to the sinusoidal vibration testing of FBGA1152 test specimen at 20°C. Measuring the diagonal board deflections at -55°C and 105°C was not feasible due to the thermal chamber. Fig. 3 shows the experimental setup and the direction considered for the out-of-plane measurements. Unlike the mechanical fatigue tests where an accelerometer was utilized, the experimental modal analysis is performed with a mass-less captor using the laser control point at the center of the board to record the velocity and determine the natural frequency of each assembly. The comparison of natural frequencies determined with both methods showed that the mass of the accelerometer had no significant influence on the results.

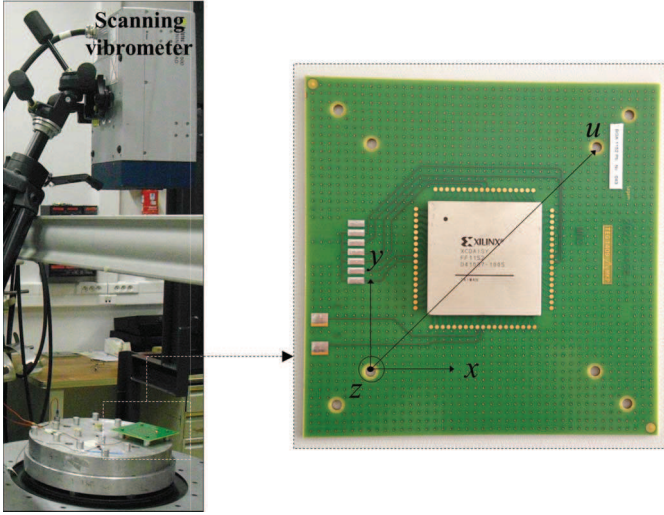


Fig. 3. Experimental setup for scanning vibrometer measurements.

Once the experimental modal deflection is obtained, the chosen method to assess damage in the critical solder ball consists in evaluating the local board curvature next to the critical solder joint [9-11]. The determination of the uniaxial deflection equation for a simple PCB (without any component) is straightforward using the boundary conditions of the system (2).

$$z(u) = \frac{d}{2} \left[1 + \sin \left(\frac{2\pi u}{a\sqrt{2}} - \frac{\pi}{2} \right) \right] \quad (2)$$

where d is the deflection at the center of the board and a is the distance between fixation points in the x and y directions. To account for the local stiffness of the board due to the FBGA1152 component, a three-parameter term (b, l, φ) is included in (2) to fit the experimental curve (3). The parameter b is related to the added local stiffness due to the component, l is related to the dimensions of the board and φ is the phase.

$$z_{b,l,\varphi}(u) = \frac{d}{2} \left[1 + \frac{\sqrt{1+b^2}}{1+b^2 \sin^2 \left(\frac{2\pi u}{l} - \varphi \right)} \cdot \sin \left(\frac{2\pi u}{l} - \varphi \right) \right] \quad (3)$$

Using the generalized reduced gradient method, (b, l, φ) can be determined for each sinusoidal loading level to match the uniaxial deflections measured with the scanning vibrometer. It turns out that the parameters remain constant regardless of the z -displacement at the center of the board: $b = 2.30 \pm 0.05$, $l = 130.79 \pm 0.64$, $\varphi = 0.61 \pm 0.01$. The mathematical formalism developed in (3) correctly captures the out-of-plane displacement of the assembly in the u -direction for a given central deflection. The local bending curvature at the location of the critical solder ball ($u = u_s$) is then calculated using the second u -derivative of (3) as depicted in (4).

$$\frac{1}{R_u(u_s)} = \kappa_u(u_s) = \left. \frac{\partial^2 z}{\partial u^2} \right|_{u=u_s} \quad (4)$$

where R_u and κ_u are respectively the radius of curvature and the curvature of the board in the u -direction. The curvature varies linearly with the central deflection (Fig. 4). The calculation shows that the bending curvature of the PCB is maximum in the areas close to the fixation points and at the locations of the critical solder joints.

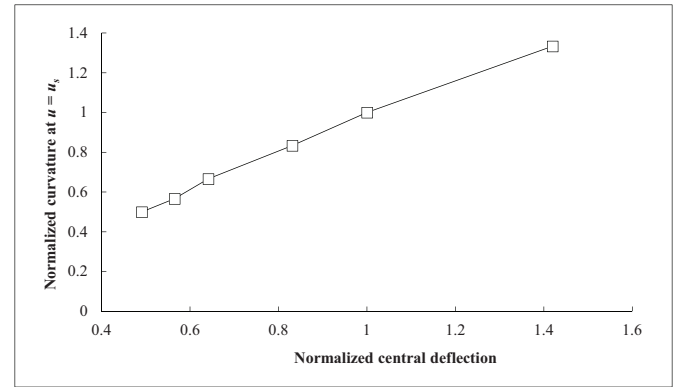


Fig. 4. Normalized curvature vs. normalized deflection.

The experimental modal deflections determined with the scanning vibrometer are then used as the fitting parameter for the finite element analysis. The accurate modeling of the first mode shape of the FBGA1152 assembly allows the accurate calculation of stress in the critical solder ball.

IV. FINITE ELEMENT ANALYSIS

The FEA is performed using ANSYS Workbench V16 software. In order to get a numerical deflection similar to the out-of-plane displacement measured with the scanning vibrometer, every material of the FBGA1152 package is accurately modeled. Considering the symmetries of the problem, 1/4th of the test board is modeled to reduce computing time. Elastic behavior is considered for the materials of the assembly and their associated properties are given in Table 2. A global-local approach using submodeling technique is used to assess the stress in the critical solder ball. Fig. 5 shows the coarse mesh of the corner ball for the global model and the fine

mesh applied for the local model. The width of the local model is equal to the solder ball pitch.

TABLE II. MATERIAL PROPERTIES AT 20°C

Material	E (GPa)	ν	ρ (g.cm ⁻³)
PCB	17	0.4	1.85
SAC305	50	0.4	7.37
Copper	124	0.33	8.96
BGA substrate	22.8	0.21	1.76
Epoxy resin	18.9	0.3	2.25
Silicon	163	0.35	2.33

First, the 3D-global model of the electronic assembly is constructed and a modal analysis is carried out to characterize its dynamic response. Natural frequency and mode shape are calculated and compared with those from experimental modal analysis. An implicit dynamic analysis is then conducted to mimic the experimental conditions of the harmonic vibration tests. One period of the input signal is simulated in order to have the desired deflection at the center of the board. Damping is not considered here since the excitation amplitude is imposed.

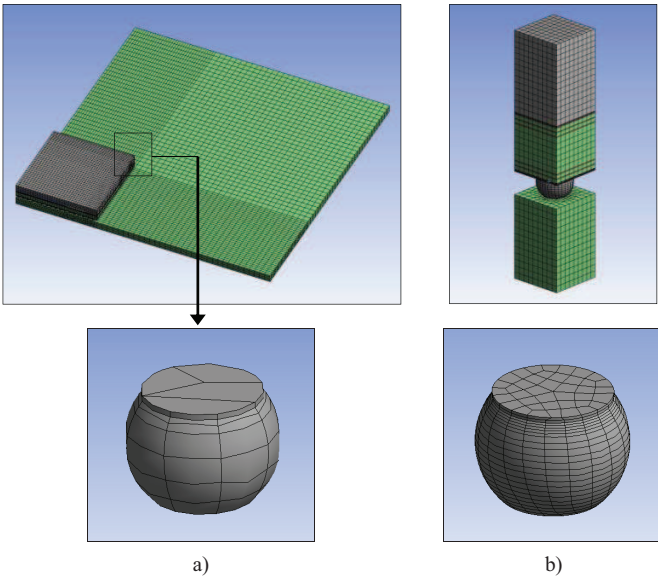


Fig. 5. Meshing of the a) global and b) local models.

The fine local model is finally used and a finite-volume-weighted averaging technique is applied to describe the stress response of the critical solder joint in a specific zone. The area of interest is chosen according to failure analysis observations. The averaging technique is used to account for meshing dependency [12]. The following equation is thus implemented in the analysis with an ANSYS command to determine the average stress in the critical solder ball:

$$\Delta\sigma_{ave} = \frac{\sum_i^n \Delta\sigma_i V_i}{\sum_i^n V_i} \quad (5)$$

where $\Delta\sigma_i$ is the stress in the i -th element, V_i the volume of the i -th element and n the number of elements in the volume of the chosen area of interest.

V. RESULTS AND DISCUSSION

A. Harmonic vibrations

As mentioned previously, each test was preceded by an experimental modal analysis to determine the natural frequency of each board. An important number of test specimens has been tested and statistical results are obtained. Fig. 6 shows the evolution of the natural frequency and the transmissibility with the temperature. The natural frequency of the test assembly increases when the temperature decreases. There is indeed an effect of the temperature on the Young modulus of the materials of the assembly and especially the glass-epoxy resin composite constitutive of the board [13]. Young modulus of FR-4 tends to increase when the temperature decreases leading to a more important global stiffness of the test assembly at low temperature. Likewise, the results show that the transmissibility, defined as the ratio of the output acceleration at the center of the board on the input acceleration of the electrodynamic shaker, is more important at high temperature. For a fixed input amplitude, the acceleration level at the center of the board decreases when the temperature decreases. From this result, and without considering thermal-induced microstructural effects on solder alloy, the curvature at the location of the critical solder ball is higher at 105°C than -55°C and it is likely to observe earlier failures at high temperature than low temperature when a constant input level is applied.

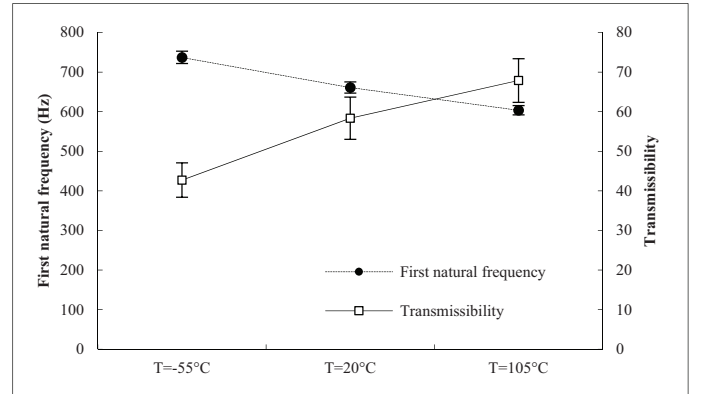


Fig. 6. Evolution of the first natural frequency and transmissibility with temperature.

The isothermal harmonic experiments have been conducted at different loading levels covering several orders of magnitude of cycles to failure (10^4 - 10^7). A two-parameter Weibull distribution is used to model the number of cycles to failure:

$$F(t) = 1 - e^{-\left(\frac{t}{\eta}\right)^\beta} \quad (6)$$

where $F(t)$ is the cumulative failure distribution function, η the characteristic life (number of cycles to failure for 63.2% of failed specimens) and β the shape parameter. Fatigue curves can therefore be plotted and the relative positioning of each curve allows the assessment of the effects of temperature and component geometry on mechanical fatigue life. The stress parameter here is not the actual stress in the critical solder

joint but rather the central z-displacement imposed on the board. Dimensions of solder joint are indeed too small to directly measure its stress strain response under vibrations. Fig. 7 gathers the fatigue curves obtained from FBGA1152 assemblies at -55, 20 and 105°C, along with those from LCC68 and PBGA324 assemblies at 20°C. It is interesting to observe that the temperature has not much effect on the durability of SAC305 solder joints under harmonic vibrations. It is also remarkable to see that the durability at 105°C is higher than the durability at -55°C. The current analysis indeed used the center deflection as the loading parameter rather than the input level. The acceleration level from the electrodynamic shaker is adjusted according to the desired displacement at the center of the board. The effect of low temperature seems to induce an embrittlement of SAC305 solder joints leading to quicker failures than those recorded at higher temperatures. Fig. 7 also shows that LCC68 and PBGA324 packages exhibit longer lifetime than FBGA1152. Size is the key parameter here since the bigger a component is, the higher the curvature near the critical solder joint is. However, LCC68 packages show better fatigue resistance than PBGA324. Even though LCC68 component is slightly bigger, the peripheral array of this component induces a lower curvature near the critical solder joint. The ball grid array produces a higher local stiffness which leads to a higher curvature next to the corner ball. Complementary scanning vibrometer measurements on LCC68 and PBGA324 will be conducted to quantify these curvatures. Further investigation is also needed to take into account solder shape effect.

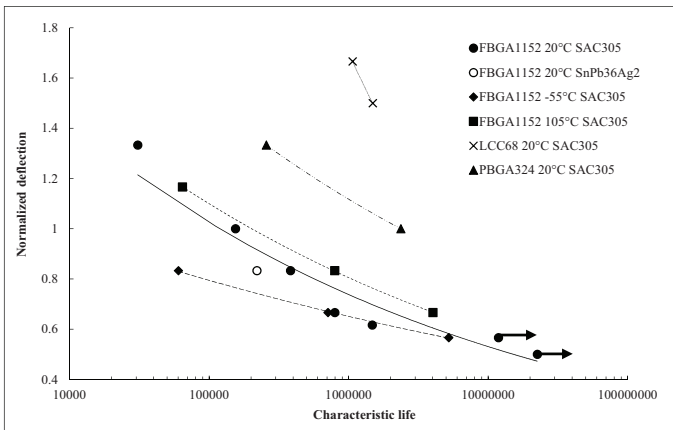


Fig. 7. Fatigue curves for FBGA1152, LCC68 and PBGA324 solder joints.

B. Failure analysis

Failure analysis was performed on failed FBGA1152 test vehicles subjected to sinusoidal vibrations at 20°C using cross-sectioning technique and microscopy observations. Three test vehicles per loading condition were cross-sectioned. A total of 109 cracks in the corner balls were observed and several failure modes were identified. Crack initiation always occurred in the solder bulk while propagation was either seen in the bulk, at the interface between the ball and the intermetallic compound (IMC) or in the IMC itself (Fig. 8). Amongst the total defects observed on the corner balls, 70% were located on the component side and 30% on the PCB side.

On the component side, 53% of the defects occurred in the solder bulk, 33% at the interface solder / IMC and 14% were ductile cracks in the IMC. On the PCB side, 15% of the defects were observed in the solder bulk, 39% at the interface solder / IMC and 45% in the IMC. Finally, pad cratering underneath the critical balls (22 occurrences) and copper trace failures (4 identified cracks) were also observed. It turns out that as the loading amplitude increases, the likelihood to observe pad cratering increases.

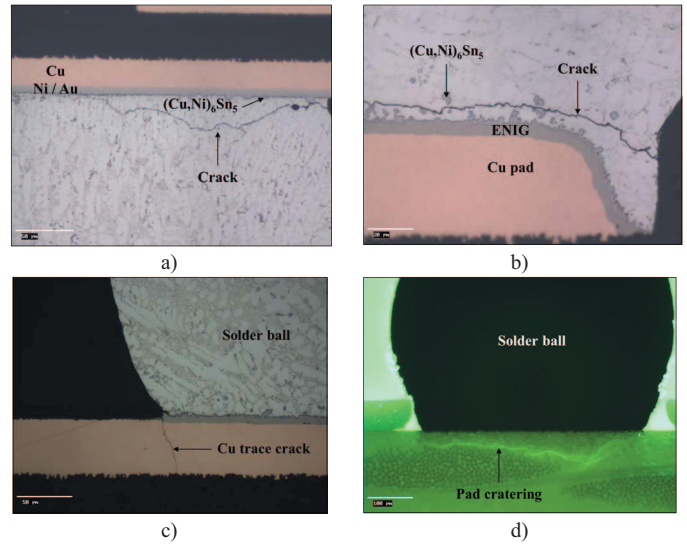


Fig. 8. Failure modes observed on FBGA1152 assembly: a) crack in the bulk on BGA side and b) PCB side, c) copper trace crack and d) pad cratering.

Failure analysis on failed assemblies at -55°C and 105°C will be conducted in order to assess the effect of temperature on SAC305 microstructure and the resulting failure modes.

C. Finite Element Analysis

The damage in the solder joint, for a specific central deflection, depends on the boundary conditions of the system. In order to assess the harmonic durability of SAC305 solder joints regardless of the boundary conditions, FEA is used to convert the central deflection into a stress fatigue criteria. The modal analysis is first performed on the global model and compared with the experimental results (Fig. 9). Equivalent Von-Mises stress in the critical area of the solder joint (five elements thick layer on BGA side) is then determined with the global-local approach and the stress-life (S-N) curve of SAC305 solder joint at 20°C can be plotted (Fig. 10).

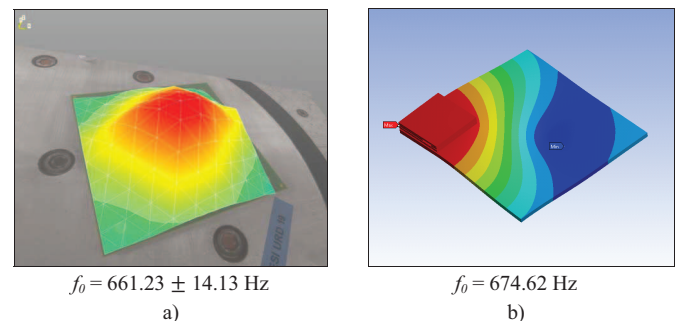


Fig. 9. a) Experimental and b) numerical first mode shape.

Vibration-induced fatigue of SAC305 solder joints can be described using Basquin's law [14]:

$$\sigma_a = \sigma_f' (2N_f)^b \quad (7)$$

where σ_a is the stress amplitude, $2N_f$ the number of reversals to failure, σ_f' the fatigue strength coefficient and b the fatigue strength exponent. The experimental data and the results from FEA are used to determine the material dependent parameters of the Basquin's law for SAC305 solder alloy.

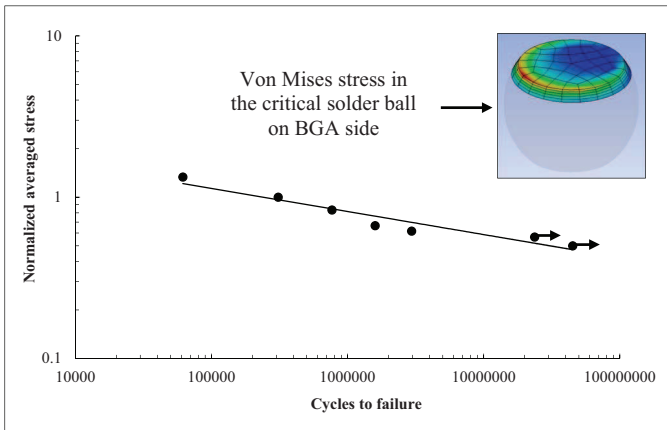


Fig. 10. Normalized log-log S-N curve for SAC305 solder joints at 20°C.

σ_f' and b fits the data points with the R^2 value of 0.9237. The difference ($\Delta\sigma_f'/\sigma_f'$, $\Delta b/b$) between the obtained model parameters and the literature is (32%, 9%) for [5], (61%, 1%) for [6] and (61%, 50%) for [15]. These scattered results are common and reveal the difficulty to develop an accurate mechanical fatigue model for solder joints.

VI. CONCLUSION

In this study, the mechanical fatigue assessment of SAC305 solder joints under sinusoidal vibrations was investigated. Isothermal fatigue tests at 20°C pointed out that SAC305 was more durable than SnPb36Ag2 solder alloy for the tested loading level. SAC305 is also more likely to fail at -55°C than 20 and 105°C due to an embrittlement at low temperature. First mode shape of FBGA1152 assembly at 20°C was experimentally determined using a scanning vibrometer and a correlation was made between the board curvature and its central deflection. A high curvature value is reached at the location of the critical solder ball indicating a high risk of solder joint failure under harmonic vibrations. A package to package comparison showed that LCC68 outperformed PBGA324 and FBGA1152 due to its peripheral array inducing a lower curvature value near the corner joint. Further investigations are nevertheless needed to assess the influence of solder shape on fatigue life. Component size is also a relevant parameter to consider when assessing the mechanical reliability of SAC305 solder joints. For the same set of boundary conditions, the bigger a component is, the higher the curvature near the critical solder joint is. FEA was then performed on FBGA1152 assembly to match experimental

first mode shape and accurately capture the stress in the corner ball. The calculated averaged von Mises stress was correlated with the experimental data in order to plot the SAC305 S-N curve at 20°C. Material parameters of the Basquin fatigue model were derived allowing the mechanical assessment of SAC305 solder joints under sinusoidal vibrations.

ACKNOWLEDGMENT

This research work was partially supported by the University of Toulouse and SAFRAN Sagem. The authors would like to thank V. Dumont for his work on the test assembly modeling and M. Bahi for his contribution regarding failure analysis.

REFERENCES

- [1] D. Steinberg, "Vibration Analysis for Electronic Equipment", 3rd edition, John Wiley & Sons, Inc. 2000.
- [2] Y.B. Kim, H. Noguchi, M. Amagai, "Vibration fatigue reliability of BGA-IC package with Pb-free solder and Pb-Sn solder", *Microelectron. Reliab.* 46:459-66, 2006.
- [3] Y.S. Chen, C.S. Wang, Y.J. Yang, "Combining vibration test with finite element analysis for the fatigue life estimation of PBGA components", *Microelectron. Reliab.* 48:638-944, 2008.
- [4] F.X. Che, J.H.L. Pang, "Vibration reliability test and finite element analysis for flip chip solder joints", *Microelectron. Reliab.* 49(6):754-760, 2009.
- [5] Y. Zhou, A. Dasgupta, "Vibration Durability Assessment of Sn3.0Ag0.5Cu & Sn37Pb Solders Under Harmonic Excitation", *Proceedings of the IMECE*, 2007.
- [6] D. Yu, A. Al-Yafawi, T.T. Nguyen, S. Park, S. Chung, "High-cycle fatigue life prediction for Pb-free BGA under random vibration loading". *Microelectron. Reliab.* 51:649-58, 2011.
- [7] T.E. Wong, B.A. Reed, H.M. Cohen and D.W. Chu, "Development of BGA Solder joint Vibration Fatigue Life Prediction Model", 49th Electronic Components & Technology Conference, San Diego, CA, , pp. 149-154, 1-4 June 1999.
- [8] B. Zhou, B. J. Qiu, and Y. F. En, "Vibration durability modeling and dynamic response analysis of pbga mixed solder joints", In *Proceedings of 11th International Conference on Electronic Packaging Technology & High Density Packaging*, pp. 616-619, 2010.
- [9] D.B. Barker, Y.S. Chen, A. Dasgupta, "Estimating the vibration fatigue life of quad leaded surface mount components", *J. Electron. Packag.* 115:195-200, 1993.
- [10] Q. Guo and M. Zhao, "Fatigue of SMT solder joint including torsional curvature and chip location optimization", *Int. J. Adv. Manuf. Technol.*, vol. 26, pp. 887-889, 2005.
- [11] R. A. Amy, G. S. Aglietti, G. Richardson, "Board-Level Vibration Failure Criteria for Printed Circuit Assemblies: An Experimental Approach", *IEEE Trans. on Electronics Packaging Manufacturing*, vol. 33, no. 4, pp. 303-311, October 2010.
- [12] L. Zhang, R. Sitaraman, V. Patwardhan, L. Nguyen and N. Kelkar, "Solder Joint Reliability Model with Modified Darveaux's Equations for the micro SMD Wafer Level-Chip Scale Package Family", *Proceedings of the 53rd. ECTC*, pp.572 -577, 2003.
- [13] R.P.L. Sanga, G.E. Ntamack, K. Mansouri, T. Beda, S.C. D'Ouazzane, "Evaluation of the mechanical characteristics of composite materials based on the Temperature. Application to Composite epoxy + glass", *J. Mater. Environ. Sci.* 4(6):1034-1041, 2013.
- [14] O.H. Basquin, "The Experimental Law of Endurance Tests", *Proc. ASTM*, 1910.
- [15] G. Limaye, "High Temperature Vibration Fatigue Life Prediction and High Strain Rate Material Characterization of Lead-Free Solders", PhD thesis, Auburn University, 2013.